Lactosome-conjugated siRNA nanoparticles for photo-enhanced gene silencing in cancer cells

Melissa Siaw Han Lim[a], Yuki Nishiyama[b], Takashi Ohtsuki[b]*, Kazunori Watanabe[b], Hirotsugu Kobuchi[a], Kazuko Kobayashi[a] and Eiji Matsuura[a,c,d]

[a]Department of Cell Chemistry, Graduate School of Medicine, Dentistry, and Pharmaceutical Sciences, Okayama University, 2-5-1 Shikata-cho, Kita-ku, Okayama 700-8558, Japan

[b]Department of Interdisciplinary Science and Engineering in Health Systems, Okayama University, 3-1-1 Tsushima-naka, Okayama 700-8530, Japan

[c]Neutron Therapy Research Centre, Okayama University, 2-5-1 Shikata-cho, Kita-ku, Okayama 700-8558, Japan

[d]Collaborative Research Centre for OMIC, Graduate School of Medicine, Dentistry, and Pharmaceutical Sciences, Okayama University, 2-5-1 Shikata-cho, Kita-ku, Okayama 700-8558, Japan

Corresponding Author*

Email: ohtsuk@okayama-u.ac.jp

Tel: +81-86-251-8218

Abstract

The A_3B-type lactosome comprised of poly(sarcosine)$_3$-*block*-poly(L-lactic acid), a biocompatible and biodegradable polymeric nanomicelle, was reported to accumulate in tumors *in vivo* via the enhanced permeability and retention (EPR) effect. Recently, the cellular uptake of lactosome particles was enhanced through the incorporation of a cell-penetrating peptide (CPP), L7EB1. However, the ability of lactosome as a drug delivery carrier has not been established. Herein, we have developed a method to conjugate the A_3B-type lactosome with ATP-binding cassette transporter G2 (ABCG2) siRNA for inducing *in vitro* apoptosis in the cancer cell lines PANC-1 and NCI-H226. The L7EB1 peptide facilitates the cellular uptake efficiency of lactosome but does not deliver siRNA into cytosol. To establish the photoinduced cytosolic dispersion of siRNA, a photosensitizer loaded L7EB1-lactosome was prepared, and the photosensitizer 5,10,15,20-tetra-kis(pentafluorophenyl)porphyrin (TPFPP) showed superiority in photoinduced cytosolic dispersion. We exploited the combined effects of enhanced cellular uptake by L7EB1 and photoinduced endosomal escape by TPFPP to efficiently deliver ABCG2 siRNA into the cytosol for gene silencing. Moreover, the silencing of ABCG2, a protoporphyrin IX (PpIX) transporter, also mediated photoinduced cell death via 5-aminolevulinic acid (ALA)-mediated PpIX accumulated photodynamic therapy (PDT). The synergistic capability of the L7EB1/TPFPP/siRNA-lactosome complex enabled both gene silencing and PDT.

Keywords

Lactosome, ABCG2, siRNA, cancer, siRNA delivery, photodynamic therapy, polymeric micelle, photosensitizer, photochemical internalization

Introduction

The discovery of RNA interference (RNAi) over two decades ago has become a promising mechanism for treating genetic diseases, including cancer, by means of altered gene expression[1-6]. In particular, small interfering RNA (siRNA) has several therapeutic advantages over conventional chemotherapeutic anti-cancer drugs. One advantage is a high specificity with minimal toxicity through siRNA-mediated gene silencing in overexpressed genes presented in recalcitrant cancer progression and metastasis[7,8]. Moreover, the versatility of siRNA due to its unlimited choice of complementary base pairing targets[9] and the sustainability of the RNA-induced silencing complex (RISC) for messenger RNA (mRNA) degradation[8] makes it a powerful tool in therapeutic applications.

However, the extensive use of siRNA clinically is encumbered by several limitations at the cellular level: an inability to readily cross biological membranes due to anionic charge; poor endosomal escape leading to cytosolic delivery failure and a lack of target specificity[4,6,10]. Moreover, following systemic administration, siRNA is physiologically unstable and susceptible to degradation by serum nucleases, renal elimination and mononuclear phagocytic system uptake[10-12]. Hence, the encapsulation of siRNA to vesicles is vital for efficient cell and systemic delivery. The successful application of siRNA for cancer therapy requires the development of both biodegradable and sustainable drug delivery system (DDS)[10-12] as the unique physiology of solid tumors bring about numerous challenges for successful therapy[4,12].

For this reason, the bioengineering of a new nanoparticle-based DDS has become the vehicle of choice for overcoming these biological barriers for many researchers[2,4,8,10,12]. Recently, a broad range of nanoparticle-based DDS (polymers, dendrimers, lipids, protein-, gold-, silica- and iron-oxide-based) has been extensively researched to promote intracellular uptake, prevent systemic degradation, and improve target specificity while reducing innate immunity responses for siRNA therapeutics[9]. Among them, polymeric conjugates and lipidic delivery systems have shown promising potential in siRNA delivery with negligible toxicity, immune and inflammatory responses and serum instability[2,10,13].

The novel polymeric micelle-type particles composed of amphiphilic polydepsipeptides, poly(sarcosine)-*block*-poly(L-lactic acid), collectively named as “Lactosome”[14], has shown superior biodegradability and biocompatibility over polyethylene glycol (PEG) liposomes[14-16]. Lactosome, with a diameter of ~35nm is a DDS carrier with promising prospects for solid tumor accumulation through the

enhanced permeability and retention (EPR) effect[16-18]. Recent studies have shown that the high hydrophilic density, tri-branched type, A_3B-type lactosome (a polymer of 3 hydrophilic polysarcosine and 1 molecule of hydrophobic polylactic acid) has an enhanced EPR effect with negligible antigenicity compared to the AB-type lactosome (one polymer of hydrophilic polysarcosine-hydrophobic polylactic acid)[15,19]. Moreover, A_3B-type lactosome stealthily evades capture by the mononuclear phagocyte system of the liver and spleen while maintaining a prolonged life time in blood circulation[17,20]. The core-shell-type micellar structure of the AB-type and A_3B-type lactosomes are composed of a hydrophobic core and inner hydrophilic cavity regions which allow further enhancement through functional modifications of the hydrophobic PLLA core. Akahoshi *et al.* had previously modified the A_3B-type lactosome with an amphiphilic EB1 type cell-penetrating peptide (CPP) and photosensitizer 5,10,15,20-tetraphenyl-21*H*,23*H*-porphyrin (TPP) to improve the *in vitro* cellular uptake and photoinduced killing ability in mammalian cancer cell lines[15]. The CPP-modified lactosome demonstrated promising properties as an efficient drug carrier but the ability to deliver hydrophilic drugs such as nucleic acids and proteins has not been studied to date.

In this study, the effect of a modified A_3B-type lactosome in gene silencing was investigated. We attempted to conjugate the ATP-binding cassette transporter G2 (ABCG2) siRNA to the previously modified A_3B-type lactosome[15] via disulfide bonds[21,22] to improve RNA stability and transfection efficiency. ABCG2, formerly known as the “breast cancer resistance protein”[23], belongs to a group of transporters capable of elucidating multidrug resistance (MDR) leading to chemotherapy failure[24]. ABCG2, ubiquitously expressed in normal tissue and overexpressed in various cancer cell lines, plays an important role in photosensitivity and phototoxicity regulation through the accumulation of porphyrin[25,26]. ABCG2 expression is inversely correlated with porphyrin derivatives in cancer cell lines and is a precursor for photodynamic diagnosis (PDD) and photodynamic therapy (PDT)[27], which provides an interesting platform for our study. PDT is a photochemical process for inducing localized tissue necrosis through the activation of a photosensitizing drug in the target tissue with light of a specific wavelength to the absorption peak of the photosensitizer in the presence of molecular oxygen to generate reactive oxygen species (ROS), including singlet oxygen ($^1O_2$)[28]. Additionally, photosensitizers have an affinity for tumor tissues compared to normal tissues and are widely used in photodynamic therapy for various types of cancers[29]. Therefore, PDT as a noninvasive therapeutic modality is a

promising candidate for clinical cancer treatment, which is based on improved therapeutic potency through combined chemotherapy-based nanomedicine and PDT[12].

Another promising strategy involving the combination of PDT and gene therapy through photochemical internalization (PCI)[30] and/or photoinduced endosomal release[31] has been widely pursued. Here, an A_3B-type lactosome was complexed with ABCG2 siRNA (siABCG2) via a disulfide exchange reaction between siRNA-SH and a surplus of PLLA-SH. Various siRNA-SH/PLLA-SH (N/P) molar ratios[5] were optimized for PLLA-SS-siRNA reaction efficiency. Subsequently, the A_3B-type lactosome was modified with CPP and photosensitizers[15] to improve the gene silencing efficiency of RNAi loaded lactosomes via enhanced cellular uptake and PCI-induced endosomal membrane disruption, respectively. The PCI strategy has been applied to release a spectrum of macromolecules such as toxins and DNA delivered within a complex of cationic polymers or adenovirus or adeno-associated viruses, dendrimer-doxorubicin conjugates, peptide nucleic acids, and bleomycin, from endosomes to the cytosol[32-37]. Furthermore, as 5-aminolevulinic acid (ALA)-mediated protoporphyrin IX(PpIX) accumulation was previously reported to correlate negatively with PpIX transporter ABCG2 expression level[27], the ALA-mediated PDT-induced cytotoxicity was evaluated in ABCG2 lactosome knocked-down cells compared with control-lactosome treated cells. Here, we have successfully developed a PLLA-SS-siRNA-lactosome polyplex conjugate loaded with CPP and photosensitizers to deliver siABCG2 into ABCG2 stably expressed human lung squamous carcinoma (NCl-H226) and human pancreatic cancer (PANC-1) cells for *in vitro* ABCG2 expression knockdown with a synergistic ALA-mediated PDT effect.

Materials and Methods

Materials

The A_3B-type amphiphilic block polydepsipeptide of (poly(sarcosine))$_3$-*block*-poly(L-lactic acid) (PSar$_{38}$)$_3$-*block*-PLLA$_{29}$, poly(L-lactic acid) PLLA blocks were similarly synthesized as described previously[19,20,38]. The poly(L-lactide), thiol terminated (PLLA-SH), protoporphyrin IX, rhodamine 6G, PLLA-NH_2, and fetal bovine serum (FBS) were purchased from Sigma-Aldrich (St. Louis, MO). The NHS-fluorescein was purchased from Thermo Fisher Scientific (Waltham, MA). The cell-penetrating peptide L7EB1 (LLLLLLLLIRLWSHLRIIHIWFQNRRLKWK) was prepared by Fmoc-based solid-phase peptide synthesis and provided by the Central Research Laboratory of Okayama University Medical School. The photosensitizer 5,10,15,20-tetrakis(pentafluorophenyl)porphyrin (TPFPP), phloxine B, 2,2'-Dithiobis(5-dinitrobenzene) (DTNP) and triethylamine were purchased from Tokyo Chemical Industry Co. Ltd. (Tokyo, Japan). *N,N*-Dimethylformamide (DMF), tetrahydrofuran (THF), 5,10,15,20-tetraphenyl-21*H*,23*H*-porphyrin (TPP), 2-mercaptoethanol (2-ME) and Ham's F12 medium were purchased from FUJIFILM Wako Pure Chemical Corporation (Osaka, Japan). 5-aminolevulinic acid (ALA) was purchased from COSMO OIL (Tokyo, Japan). Tris[2-carboxyethyl] phosphine (TCEP), 3-(4,5-dimethylthiazol-2-yl)-2,5-diphenyltetrazolium bromide (MTT) and Dulbecco's modified Eagle's medium (DMEM) were purchased from Nacalai Tesque (Kyoto, Japan). Human targeting thiol modified ABCG2 siRNA (siABCG2) (sense: 5'- HS-C_6-GGACUAGUAUAGGAAUGGATT-3', antisense: 5'-UCCAUUCCUAUACUAGUCCTT-3') and scramble siRNA (siScr) (sense: 5'-HS-C_6-GUGACUGAUAGAGAGAUAGTT-3', antisense: 5'-CUAUCUCUCUAUCAGUCACTT-3') were purchased from Japan BioServices Co. Ltd. (Saitama, Japan). All other chemicals were of analytical grade and obtained from Nacalai Tesque.

Cell line

The NCl-H226 human lung cancer cell line and PANC-1 human pancreatic carcinoma cells were purchased from the American Type Culture Collection (Manassas, VA). Chinese hamster ovary (CHO) cells (FLIP-In cell line) were purchased from Invitrogen (Waltham, MA).

Preparation of PLLA-SS-siRNA

The polylactic acid (PLLA) in DMF was prepared by drying 2 µL of 1 mM PLLA-SH in DMF [pre-treated with 500 mM 2-ME] (2 nmol) solution in a centrifugal vacuum dryer for 5 h to completely remove the 2-ME. Then 40 µL of DMF was added to the pellet to dissolve the PLLA (100 µM). The siABCG2 was prepared by mixing [20 µL of 50 µM (5')HS-C_6-siRNAsense, 20 µL of 50 µM siRNA antisense and 10 µL of 5x annealing buffer (100 µM HEPES-KOH buffer (pH 7.4), 10 µM Magnesium Acetate)]. This mixture was then heated with a PCR machine at 90˚C for 1 min and gradually cooled to 4˚C at a rate of 1˚C/s to produce double stranded siRNA. Thereafter, 5.5 µL of 10 mM TCEP was added to the solution, mixed and incubated at 37˚C for 1 h. After incubation, purification of the RNA by ethanol precipitation was performed by adding 5.5 µL (1/10 of precipitation quantity) of 3M sodium acetate buffer (pH 5.2), vortexed, and followed by the addition of 153 µL (2.5 times volume of precipitation quantity) of cold 100% ethanol and vortexed.

The mixture was cooled overnight at -80˚C. After that, the mixture was centrifuged at 15,000 rpm, 4˚C for 15 min and the supernatant was removed. Next, 150 µL of 85% cold ethanol was added to the precipitate and centrifuged again at 15,000 rpm, 4˚C for 5 min and the supernatant was removed. Finally, 50 µL of RNase free water was added to dissolve the precipitate to produce 20 µM of HS-C_6-siRNA. A 10% PAGE solution was used to confirm the TCEP treated RNA.

Nitropyridine-SS-siRNA was prepared by mixing [20 µL of 20 µM HS-C_6-siRNA (400 pmol), 2 µL of 10 mM DTNP in THF (20 nmol), 18 µL THF], vortexed and incubated at 25˚C for 24 h under constant stirring. The solution was then dried up with a centrifugal vacuum dryer to produce dried pale yellow nitropyridine-SS-siRNA. To remove the excess DTNP, 40 µL of RNase free water and 120 µL of chloroform was added to the pellet and vortexed. The solution was centrifuged at 15,000rpm, 4˚C for 5 min and the water layer was transferred to a new 1.5 ml tube and dried with a centrifugal vacuum dryer to produce DTNP-free-nitropyridine-SS-siRNA. The conjugation of PLLA-SS-siRNA was performed by mixing the prepared 50 µM PLLA-SH in DMF (40 µL) solution to the dried DTNP-free-nitropyridine-SS-siRNA, vortexed and incubated at 40˚C for 12 h under constant stirring.

Preparation of lactosome complexes incorporating PLLA-SS-siRNA, L7EB1 and photosensitizer

A chloroform solution containing the $(PSar_{38})_3$-*block*-$PLLA_{29}$ (40 nmol, 3.1 μg) with 1 mol% of TPFPP,12.5 mol% of L7EB1 which contains a cysteine residue at its C-terminus and 1 mol% of PLLA-SS-siRNA was added to the glass test tube. Saline (360 μL) was then added to the test tube, gently vortexed and placed at room temperature for 30 min. This lactosome mixture was then passed through a 0.1 μm syringe filter (Membrane Solutions, Dallas, TX) to remove large aggregates before diluted with 350 μL of T-buffer (20 mM HEPES-KOH buffer (pH7.6), 115 mM NaCl, 5.4 mM KCl, 1.8 mM $MgCl_2$, 13.8 mM glucose). Low molecular weight molecules were excluded from the mixture using Amicon Ultra-0.5 (MWCO 100 kDa, Merck Millipore, Darmstadt, Germany). To analyse the concentrations of siRNA, L7EB1, TPFPP and absorption spectra of the lactosome, complexes were measured using a UV-Vis spectrophotometer (DeNovix, Wilmington, DE, USA).

To fluorescently label the lactosome complex, 0.5 mol% of PLLA-fluorescein was added to the initial mixture of constituents (the chloroform solution) described above. The PLLA-fluorescein was prepared as follows: PLLA-NH_2 (50 nmol) dissolved in 100 μL of dimethylformamide / triethylamine (100:1) was added to dried NHS-fluorescein (50 nmol). This mixture was reacted at 37˚C for 4 h. The encapsulation method used for the other photosensitizers (TPP, protoporphyrin IX, phloxine B, and rhodamine 6G) was the same as for the TPFPP described above.

Particle size distribution and ζ-potential

The particle size, size distribution, polydispersity index (PDI), and ζ-potential were measured by Zetasizer Nano ZSP (Malvern Instruments, Malvern, Worcestershire, UK) using the dynamic light scattering (DLS) method. All measurements were performed at a fixed angle of 90˚ and at 25˚C room temperature. The results were expressed as the size (mean ± SD).

Loading efficiency

Loading efficiency for the L7EB1 was calculated after measuring the absorption spectrum according to the formula below.

$$\text{L7EB1 loading efficiency} = \frac{\text{A280} \times \text{volume} \div \Sigma 280(\text{L7EB1})}{\text{Initial amount of CPP (10 nmol)}} \times 100$$

where A_{280} is A_{280} (CPP loaded lactosome) – A_{280} (blank lactosome); volume is that of the final volume of the lactosome solution.

A similar method at 411 nm for photosensitizer TPFPP and 260 nm for siRNA was used to calculate both photosensitizer and siRNA loading efficiency.

Evaluation of cellular uptake of the lactosome complexes including various photosenstizers

CHO cells were cultured at 37°C under 5% CO_2 in Ham's F12 medium supplemented with 10% FBS, 100 units/ml penicillin and 100 μg/ml streptomycin. The cells were seeded at a density of 2×10^4 cells/well in a 96-well plate and incubated at 37°C under 5% CO_2 overnight. The cells were then incubated at 37°C for 3 h with the lactosome carrying L7EB1 and a photosensitizer (TPFPP, TPP, protoporphyrin IX, phloxine B, or rhodamine 6G) dissolved in a 200 μL T-buffer. The lactosome solution was exchanged for Ham's F12 medium before irradiation. The cells treated with TPFPP, TPP and protoporphyrin IX were irradiated at 400 – 440 nm (5 J/cm^2), and the cells treated with phloxine B and rhodamine 6G were irradiated at 530-550 nm (5 J/cm^2). The cellular fluorescence images were obtained by fluorescence microscopy using an IX51 microscope (Olympus, Tokyo, Japan).

Lactosome complex induced ABCG2 knockdown

Cells were cultured in complete medium DMEM supplemented with 10% FBS, 100 units/ml penicillin and 100 μg/ml streptomycin and incubated at 37˚C under 5% CO_2. Typically, cells were seeded on a multi-well plate and cultured in the conditioned medium until confluent. The cells were then seeded at a density of 2×10^4 cells/well in a 96-well plate and incubated at 37˚C under 5% CO_2 for 24 h. The cells were then incubated at 37˚C for 5 h with L7EB1/TPFPP/siRNA-lactosome (PLLA-PSar$_3$ 10 nmol, TPFPP 1.25 mol%, L7EB1- 12.5 mol%, PLLA-SS-siRNA 0.25 mol%) dissolved in DMEM. The cells were then irradiated at 405 nm at 45-50 mW/cm^2 for 20 s (1.85 – 2.0J/cm^2). Alternatively, the cells were incubated at 37˚C for 5 h with empty lactosome as a control as well as L7EB1/TPFPP/siABCG2-lactosome, L7EB1/TPFPP/siScr-lactosome, TPFPP/siABCG2-lactosome and L7EB1/siABCG2-lactosome formulations with or without irradiation (405 nm, 45-50 mW/cm^2 for 20 s). Then, the cell

medium was exchanged for 10% FBS supplemented DMEM medium and incubated for 48 h for gene knockdown.

Quantitative analysis of mRNA expression (*In vitro* ABCG2 silencing)

RNA was extracted with NucleoSpinRNA Plus Kit (Macherey-Nagel, Düren, Germany) and the concentration of isolated RNA was measured with BioSpec-nano Spectrophotometer (Shimadzu Co. Ltd., Kyoto, Japan). Then, RNA was converted to cDNA with ReverTra Ace qPCR RT Master Mix with gDNA Remover (Toyobo Co. Ltd., Osaka, Japan) for further analysis of mRNA expression. ABCG2 mRNA levels were measured in transfected NCI-H226 and PANC-1 cells by real-time PCR (RT-PCR) analysis using TaqMan Gene Expression Assay Primers (ABCG2, Hs01053790_m1) and (ACTB, Hs01060665_g1) (Thermo Fisher Scientific, Rockford, IL) and TaqMan Fast Advance Master Mix run on StepOnePlus v2.3 (Applied Biosystems, Rockford, IL). The PCR cycling conditions were: 2 min preincubation at 50˚C, 21 s denaturation at 95˚C, 20 s annealing at 60˚C for 40 cycles. The results were normalised to *ß*-actin. The results were expressed as threshold cycles (Ct). The relative quantification of the target transcripts was determined by the comparative Ct method (ΔΔCt) according to the manufacturer's protocol. The $2^{-\Delta\Delta Ct}$ method was used to analyse the relative changes in gene expression.

Photodynamic treatment

Cells were seeded at a density of 2×10^4 cells/well in a 96-well plate and incubated for 24 h at 37˚C. The cells were then incubated at 37˚C for 5 h with L7EB1/TPFPP/siRNA-lactosome (PLLA-$PSar_3$ 10 nmol, TPFPP 1.25 mol%, L7EB1- 12.5 mol%, PLLA-SS-siRNA 0.25 mol%) dissolved in DMEM. The cells were then irradiated at 405 nm, 45-50 mW/cm^2 for 20 s (1.85 – 2.0J/cm^2). Alternatively, the cells were incubated at 37˚C for 5 h with empty lactosome as a control as well as L7EB1/TPFPP/siABCG2-lactosome, L7EB1/TPFPP/siScr-lactosome, TPFPP/siABCG2-lactosome and L7EB1/siABCG2-lactosome formulations with and without irradiation (405 nm, 45-50 mW/cm^2 for 20 s). Then, the cell medium was exchanged for 10% FBS supplemented DMEM medium and incubated for 48 h before conducting the ALA-PDT treatment. For the ALA-PDT treatment, the cells were incubated for 3 h with

1 mM ALA in complete medium. The cells were then exposed to light (40 mW/cm^2) for 10 minutes using a Na-Li lamp (TheraBeam VR630, Ushio Inc., Tokyo, Japan) at a wavelength of 630 nm[27,39]. Then, the cells were further cultured for 24 h and cell survival was determined using an MTT assay.

Cell viability assay using 3-(4,5-dimethylthiazol-2-yl)-2,5-diphenyltetrazolium bromide (MTT)

Cells were incubated for 0.5 h with a culture medium containing 0.125 mg/ml MTT at 37°C. The insoluble end product (formazan derivatives) was solubilised in 150 µL dimethyl sulfoxide (DMSO) after removing the medium. The absorbance at 570 nm was measured using a microplate reader (Tecan Sunrise, Männedorf, Switzerland). Cell survival was expressed as a percentage of the control.

Statistical analysis

All results were expressed as mean ± SD. Differences between groups were assessed by the Student' *t*-test for independent samples. *P* values of <0.05 were considered statistically significant.

Results and Discussions

PLLA-SS-C_6-siRNA synthesis

The covalent conjugation of siRNA to polymer carriers via the thiol modified sense strand added at the 6-carbon chain to the 5'end terminal has superior stability *in vivo* over conventional siRNA polyplexes formed by electrostatic interactions[40]. As part of our long-term plan to develop lactosome-base nanocarriers for siRNA delivery, we adopted the siRNA conjugation strategy to efficiently deliver siRNA into cells. The PLLA-SS-C_6-siRNA component was synthesised over a two-step process (Figure 1(a)). A large excess, 20 nmol of DTNP in THF was added to the thiol modified, TCEP treated siRNA, HS-C_6-siRNA under constant stirring to ensure all the HS-C_6-siABCG2 participated in the thiol exchange with DTNP. Prior to the PLLA-SH conjugation, the annealed thiol modified siRNA was treated with 10 mM of TCEP to cleave the disulfide bonds between the sense strand of siRNA (Fig. S1). Here, the S-S bonds on the thiol modified siRNA could be reduced into SH groups. This prevents the thiol modified siRNA from being oxidised before the disulfide formation reaction.

The conjugated compound of PLLA-SS-C_6-siRNA was prepared by adding a 1:5 mole ratio of HS-siRNA:PLLA-SH. The 2-ME treated PLLA, PLLA-SH was diluted in DMF and added to the dried DTNP-free-nitropyridne-SS-C_6-siRNA under constant stirring to facilitate the reaction. Here, we expected the excess PLLA-SH to replace all the nitropyridine groups of HS-siRNA through covalent bonding. We deduced that assembling the bioreducible hydrophobic PLLA-SH with 5'-thiol functionalized siRNA would lead to the rapid formation of stable conjugate polyplexes by thiol-disulfide exchange reaction because of the local high concentration of the disulfides and thiols within the polyplexes. This thiol exchange reaction allows the negatively charged hydrophilic siRNA to be modified into a hydrophobic entity to enable lactosome conjugation through the modifiable hydrophobic PLLA core of the lactosome complex. The prerequisite for the success and usefulness of amphiphilic gene carriers is to efficiently form polymer/siRNA complexes, a process that can be confirmed by the retardation of siRNA mobility in Native 10% PAGE analysis. The covalent PLLA-SS-C_6-siRNA complexes formed were able to retard siRNA mobility in gels as shown in Figure 1(b). Here, the HS-C_6-siRNA band can be seen near the 25 bp position of the DNA marker, while the PLLA-SS-C_6-siRNA band was shifted due to the weight of the modified PLLA-SH conjugated siRNA. It is worth noting that for the PLLA-SS-C_6-siRNA band, a faint band near the 25 bp position was still visible, indicating the

presence of free HS-C_6-siRNA or unreacted nitropyridne-SS-C_6-siRNA, most likely from partial siRNA-SH oxidation. However, it is safe to assume that the unreacted nitropyridne-SS-C_6-siRNA is negligible and almost all nitropyridine groups have been covalently replaced by the excess PLLA-SH. However, the retardation was complete only when an excess (5 times) of PLLA-SH polymer was present.

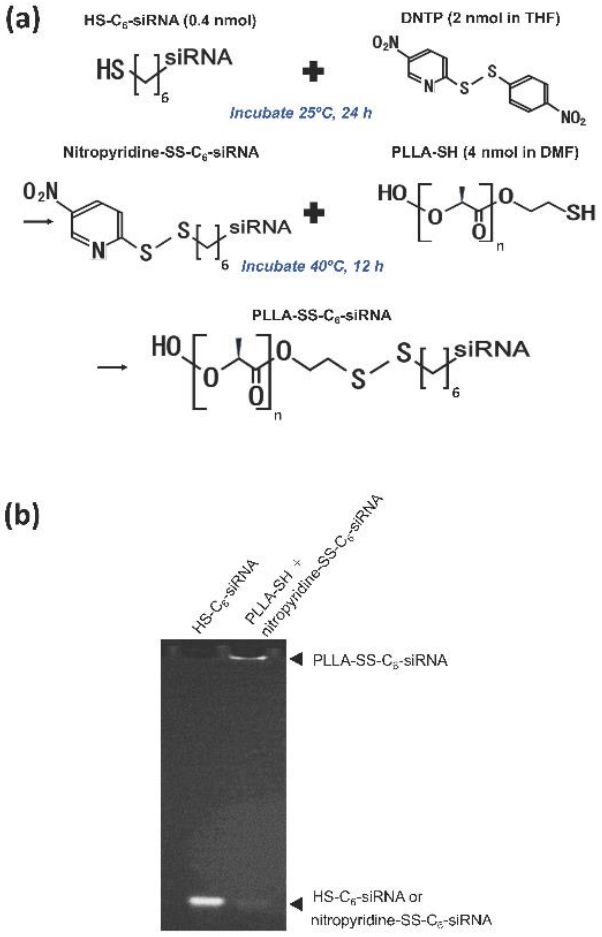

Fig. 1. (a) Synthesis of PLLA-SS-siRNA (thiol exchange reaction between HS-C_6-siABCG2 and DTNP) and (the reaction between Nitropyridine-SS-C_6-siRNA and PLLA-SH). (b) Native 10% PAGE analysis of HS-C_6-siRNA and PLLA modified siRNA (ethidium bromide staining).

Photo-induced cytosolic dispersion

Utilizing more than one stimulus can increase drug delivery efficiency, and several multiple stimuli-responsive drug delivery nanoparticles have been established such as the combination of a pH and

redox stimuli[12,41]. The acidic pH in endosomes and lysosomes triggers the drug release in tumors while the redox responsiveness is triggered in the cytoplasm which contains a high concentration of GSH[42,43]. However, engineering a stepwise multiple stimuli-responsive nanocarrier with efficient pH buffering capacity capable of recognizing and dynamically responding to different microenvironments remains a great challenge[12,30,43]. Polycations that possess the required buffering capacity may demonstrate high *in vitro* transfection efficiency through the postulated proton sponge effect, but their intrinsic cytotoxicity is a possible impediment to their clinical utility as gene carriers. Moreover, the same pH distribution shared inside normal and tumor cells complicates the realization of specific siRNA release by acidic pH endosomes[43]. Therefore, an alternative strategy utilizing the encapsulation of a photosensitizer into nanoparticles coupled with enhanced cellular uptake efficiency via a cell penetrating peptide has been pursued recently. This strategy enables active targeting and controlled drug release via short-time light irradiation or PCI[12,43]. The photosensitizer energizes the surrounding molecular oxygen ($^3O_2$) to generate reactive oxygen species (ROS), which inadvertently induces lipid peroxidation facilitating endosomal escape. This presents great potential in enhancing therapeutic efficacy and minimizing off-target effects[12]. It was established that the EB1 cell penetrating peptide showed superior cellular internalization for photosensitizer-loaded lactosomes[15], which accumulated in the endosomes/lysosomes. To assess whether the L7EB1 conjugated lactosome carrying photosensitizers could disrupt the endosomal/lysosomal membrane and hence facilitate gene escape from the lysosomes after irradiation, the PCI effect of photosensitizer-complexed L7EB1-modified lactosome and its subsequent photo-induced cytosolic dispersion was observed by fluorescence microscopy. The affinity of photosensitizers towards plasma membrane localization via hydrophobic-hydrophobic interactions is vital in improving the cytosolic release of macromolecules trapped in the endosomes/lysosomes in a light-inducible manner[30].

Figure 2 shows the internalization of L7EB1-modified lactosome by various photosenstizers (TPFPP, TPP, protoporphyrin IX, phloxine B and rhodamine 6G) in CHO cells. The photosensitizer-complexed L7EB1-modified lactosomes were added to CHO cells and incubated at 37°C for 3 h before short photoirradiation. After irradiation, the green spots increased with a fluence of 5 J/cm^2 in the cells treated with the TPFPP- or TPP-complexed L7EB1-lactosomes. These results showed that the endocytosed L7EB1/TPFPP- and L7EB1/TPP-lactosomes, which accumulated in the endosomes/lysosomes, could destabilize the endosomal/lysosomal membranes causing a rapid

cytosolic fluorescence increase in treated cells. By contrast, after irradiation with a fluence of 5 J/cm^2, the cells treated with the protoporphyrin IX-, phloxine B- or rhodamine 6G-complexed L7EB1-lactosomes showed no significant observable cytosolic fluorescence increase. This indicated that both TPFPP- and TPP-complexed L7EB1-lactosomes can efficiently escape from endosome encapsulation via short photoirradiation (Fig. S2). Compared to TPP, TPFPP-complexed L7EB1-lactosome showed higher cytosolic fluorescence intensity after irradiation, indicating that TPFPP is a superior photosensitizer for PCI-dependent cytosolic delivery of the lactosome complex. This showed that siRNA transfection efficiency can be improved through TPFPP conjugation to facilitate siRNA delivery as it will trigger the escape of siRNA from the endosomal region to the cytoplasmic region of the cells to exhibit its gene silencing effect.

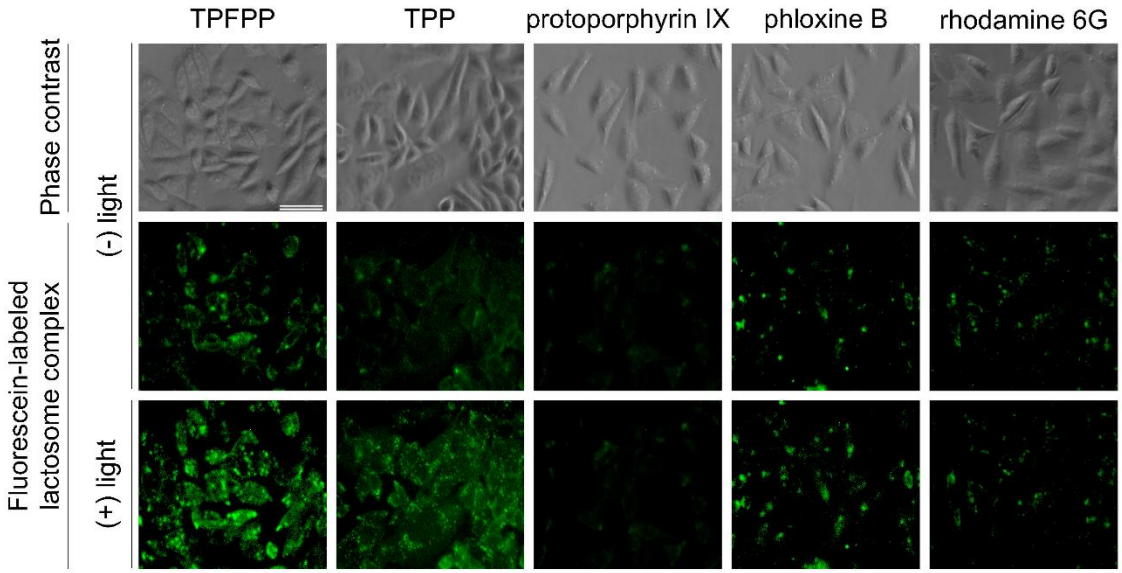

Fig. 2. Photoinduced cytosolic dispersion of L7EB1/photosensitizer-lactosome including PLLA-fluorescein (0.5 mol% of the lactosome polymer). The lactosome complexes were shown by the fluorescein images. CHO cells were irradiated at 400-440 nm (5 J/cm^2) for TPFPP, TPP and protoporphyrin IX, and at 530-550 nm (5 J/cm^2) for phloxine B and rhodamine 6G. Scale bar, 50 μm.

L7EB1/TPFPP/siRNA-lactosome complex

The siRNA-loaded lactosome, including TPFPP and EB1 cell-penetrating peptide, was prepared by the injection method as described in the Materials and Methods section. EB1 cannot assemble into the

lactosome particles. Thus, in our previous study[15], EB1 bearing a C-terminal Cys residue was reacted with maleimide-PSar-PLLA, and the modified EB1 having hydrophobic PLLA moiety was used for its assembly into the hydrophobic core of lactosome particles. Instead of such laborious EB1/PSar-PLLA conjugation, we found in this study that the simple addition of hydrophobic $(Leu)_7$ residues to EB1 peptide (the use of L7EB1) enables its assembly into the lactosome particles.

The lactosome complex formation was slightly modified from the previously established film method[15]. The film method (results not shown) was thought to be inferior because of the tendency for the PLLA-SS-C_6-siRNA to form aggregates and hence not incorporated into the hydrophobic core of the lactosome at the time of lactosome formation. In addition, the L7EB1 also formed aggregates with PLLA-SS-C_6-siRNA, causing suboptimal conjugation of both L7EB1 and siRNA into lactosomes and was instead removed during the 100 kDa ultrafiltration procedure. By directly incorporating the PLLA-SS-C_6-siRNA into lactosomes, the modified nucleic acid, PLLA-SS-C_6-siRNA is thought to be incorporated into the lactosome via hydrophobic interactions between PLLA moiety and the hydrophobic core of the lactosome resulting in the formation of siRNA-loaded lactosome (siRNA-lactosome). The cell penetrating peptide L7EB1 on the other hand was expected to be assembled into the lactosome particles by the interaction of the L7 moiety with the hydrophobic core, while the photosensitizer, TPFPP, was to be encapsulated in the hydrophobic core of the lactosome by hydrophobic interaction[15], forming the siRNA loaded L7EB1/TPFPP-lactosome complex (L7EB1/TPFPP/siRNA-lactosome). The only drawback of this method is that by using impurified PLLA-SS-C_6-siRNA, the free unconjugated PLLA-SH may to a certain extent be incorporated into the lactosomes, hence making it difficult for to exactly quantify the amount of PLLA-SS-C_6-siRNA conjugation. Furthermore, the PSar-PLLA absorption peak of 230 nm[15] complicates the process.

To confirm the incorporation of siRNA, L7EB1 and TPFPP into the lactosomes, the loading efficiency of successfully conjugated L7EB1/TPFPP/siRNA-lactosome complex was analysed using a UV-Vis spectrophotometer as shown in Figure 3(c). The max absorbance wavelengths for siRNA, L7EB1 and TPFPP were identified as 260 nm, 280 nm and 411 nm[15], respectively. The loading efficiency for each component incorporated in the lactosome was then calculated as previously described in the Materials and Methods section. A loading efficiency between 50%-70% for each incorporated siRNA, L7EB1 and TPFPP was found to be relatively stable with optimal transfection

results. The reason for this may be due to the equally incorporated proportions for each component into the $PLLA_{29}$ of the lactosome, which stabilises the complex. However, as the PSar-PLLA absorption peak was reported to be around 230 nm, we were unable to determine the exact loading efficiency of incorporated siRNA (with an absorption peak of 260 nm). A more effective quantitative method is warranted for future studies.

A schematic illustration of the conjugation is depicted in Figure 3(a). There is a strong relationship between the physiological properties of nanoparticles with their capacity to complex with and deliver siRNA into cell cytosol. The cellular uptake efficiency of the lactosomes modified with amphipathic CPPs such as L7EB1 was higher than that of unmodified lactosomes. These modified lactosomes also successfully delivered the hydrophobic photosensitizer TPP into cells, inducing cell death through PDT experiments[15].

We proposed that the bioreducible hydrophobic $PLLA_{29}$ core of the polymeric $(PSar_{38})_3$-*block*-$PLLA_{29}$ lactosome plays a major role in functional modifications through the internalization of various hydrophobic-modified cargo molecules. The loading capacity and type of cargo incorporation of the hydrophobic core inadvertently affects the size and charge of the lactosome carrier. The mean ± SD hydrodynamic particle size (nm) for L7EB1/TPFPP/control-lactosome (without siRNA) complex and L7EB1/TPFPP/siRNA-lactosome complex was 37.03 ± 2.11 nm and 50.44 ± 1.08 nm, with a PDI of 0.28 ± 0.01 and 0.27 ± 0.03, respectively. The mean ± SD ζ-potential value of L7EB1/TPFPP/control-lactosome complex was -1.14 ± 1.14 mV and for L7EB1/TPFPP/siRNA-lactosome complex was -1.96 ± 0.35 mV. Compared to the previously EB1 CPP incorporated lactosome which showed an average diameter of 38 ± 0.2 nm and a ζ-potential of 1.6 ± 0.3 mV[15], the decrease in ζ-potential seems to be due to the negatively charged siRNA molecules. These results demonstrated that the modification of lactosome with siRNA decreases their surface charge while increasing the particle size. Despite the negative charge, the complex demonstrated significant ABCG2 knockdown efficiency in PANC-1 and NCI-H226 cells as is shown in Figure 4. One of the reasons may be attributable to the amphiphilic nature of the lactosomes augmented by the incorporated CPPs. Previous studies also reported that nanoparticles 60-80 nm in size favour the caveolae mediated endocytosis pathway which bypasses lysosomes[44,45]. Therefore, controlling the CPP-conjugated lactosome particle size may also facilitate

cellular uptake efficiency. Moreover, the lactosome complex with a slight negative ζ-potential value will likely not interact with the negatively charged cell membranes, leading to reduced cytotoxic effects during the long incubation period.

Figure 3(b) shows the cellular uptake of L7EB1/TPFPP/siRNA-lactosome complexes coupled with short photoirradiation to promote endosomal escape and release of the siRNA into cytosol to exhibit its gene silencing effect. Short photoirradiation or PCI is a specific branch of PDT utilized for the site-specific release of membrane-impermeable macromolecules into the cytosol of target cells. The concept of PCI is based on the breakdown of the endosomal/lysosomal membranes through the photoactivation of photosensitizers that accumulate on the membranes of these organelles[46]. Here, we demonstrated a synergistic effect of L7EB1/TPFPP/siRNA-lactosome complex cellular uptake enhancement by L7EB1 followed by TPFPP-PCI endosomal destabilization to release the conjugated siRNA from the lactosome complex into the cytosolic component of cancer cells.

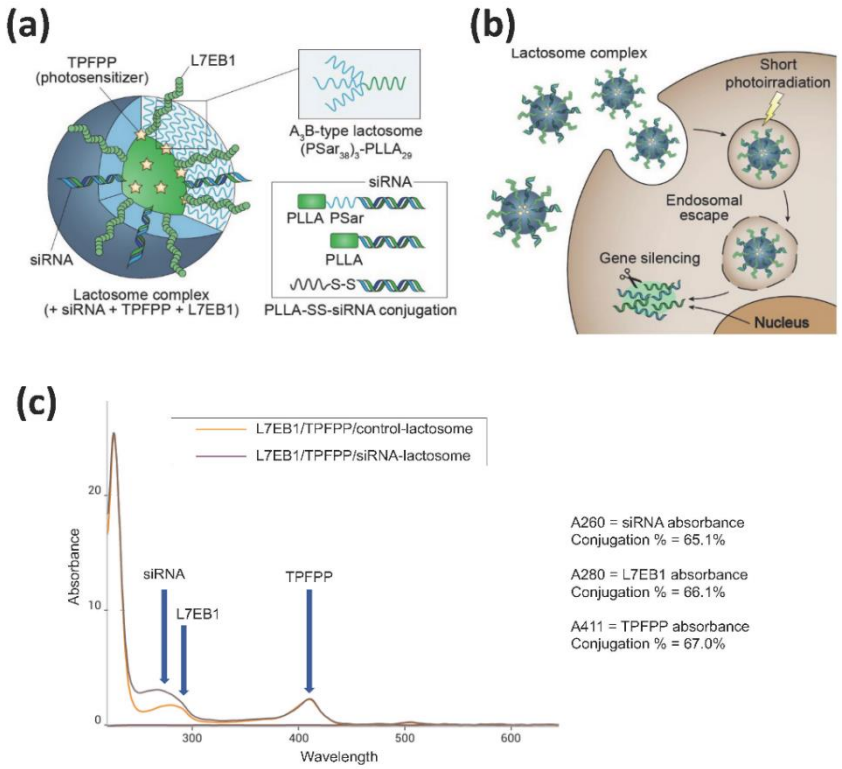

Fig. 3. (a) Schematic illustration of L7EB1/TPFPP/siRNA-lactosome particles. (b) The internalization of the siRNA-lactosome complex via enhanced cellular uptake using L7EB1 and endosomal escape via short photoirradiation (405 nm at 45-50 mV/cm^2 for 20 s). (c) Loading Efficiency of incorporated siRNA, L7EB1 and TPFPP (UV-Vis spectrophotometer).

ABCG2 knockdown with L7EB1/TPFPP/siRNA-lactosome

To evaluate the transfection efficiency of the L7EB1/TPFPP/siRNA-lactosome complexes with or without irradiation at non-toxic conditions, 0.4 nM of TPFPP was used with a fluence of 1.8 J/cm^2. The ABCG2 gene silencing effects of L7EB1/TPFPP/siABCG2-lactosome complexes was evaluated on the stably expressed ABCG2 cancer cells PANC-1 and NCI-H226. RT-PCR was used to quantify the efficiency of the ABCG2 knockdown at the mRNA level. Figure 4 shows the knockdown efficiency for the cell lines tested in this study. For each cell line, the mRNA expression levels were measured following treatment with different formulations of lactosome complexes and were compared to the control-lactosome complex treated cells after a short photoirradiation. The relative ABCG2 expressions (mean ± SD) using conjugated L7EB1/TPFPP/siABCG2-lactosome (with photoirradiation) complex in the PANC-1 and NCI-H226 cells were 23.9 ± 8.6% and 15.6 ± 3.7%, respectively, which were significantly lower than those in the control-lactosome complex treated cells (p=0.004 and p=0.001, respectively). Moreover, the relative ABCG2 expressions in L7EB1/TPFPP/siScr-lactosome (with photoirradiation) complex treated PANC-1 and NCI-H226 cells were 101.3 ± 36.6% and 95.0 ± 4.6%, respectively, compared to the control-lactosome complex treated cells (p=0.955 and p=0.199, respectively), confirming the specific gene silencing action of the siABCG2.

The knockdown efficiency of L7EB1/TPFPP/siABCG2-lactosome complex treated cells (without photoirradiation) and TPFPP/siABCG2-lactosome complex (with photoirradiation) treated cells were not significantly different from the control-lactosome complex treated cells in both PANC-1 and NCI-H226 cells. The relative ABCG2 expressions for L7EB1/TPFPP/siABCG2-lactosome (without photoirradiation) complex treated PANC-1 and NCI-H226 cells were 102.7 ± 5.8% and 108.0 ± 2.0%, respectively, compared to the control-lactosome complex treated cells (p=0.508 and p=0.020, respectively). Whereas the relative ABCG2 expressions for TPFPP/siABCG2-lactosome (with photoirradiation) complex treated PANC-1 and NCI-H226 cells were 158.3 ± 8.6% and 106.3 ± 7.4%, respectively, compared to the control-lactosome complex treated cells (p=0.007 and p=0.275, respectively), This proved that the application of PCI improved the cytosolic release of siABCG2 from the endosome/lysosome entrapment in a light-inducible manner for efficient ABCG2 gene silencing in both PANC-1 and NCI-H226 cells. Porphyrin-based photosensitizers demonstrated superior endocytic

membrane localization with low aggregation in the cell compartment, leading to highly localized and focused light-dependent activation with high specificity. These characteristics limit the biological effect to only the illuminated areas, which minimalizes potential systemic side effects of the therapeutic nanomolecules[29]. Moreover, studies have reported that upon transfection, a porphyrin conjugated dendrimer may be dissociated from conjugated genes in endosomes/lysosomes and subsequently translocated to the endosomal/lysosomal membranes due to the hydrophobicity nature of the porphyrin used. This condition not only prevented phototoxicity, as the porphyrin does not induce dark toxicity, but it could also prevent photochemical damage to the genes used and hence deliver a more efficient transfection[47,48]. In this study, we proposed that the TPFPP, covalently bound to the biodegradable lactosome complex, should be dissociated and translocated to the endosomal/lysosomal membrane once it successfully progresses into endosomes/lysosomes to prevent photochemical damage to the siRNA and satisfying the requirements for effective PCI-mediated gene delivery (Fig. S2).

We have confirmed that although the incorporation of L7EB1 into lactosomes may enhance the cellular uptake mechanism, it is insufficient to deliver siRNAs into cytosols for gene silencing. The relative ABCG2 expressions for L7EB1/siABCG2-lactosome (without photoirradiation) complex treated PANC-1 and NCI-H226 cells were 120.0 ± 14.0% and 127.0 ± 22.5%, respectively, compared to the control-lactosome complex treated cells (p=0.132 and p=0.173, respectively). With L7EB1 alone, the complexes may be endocytosed and trapped into the endosomes/lysosomes without the ability to escape and release the siRNA content into the cytosol for gene knockdown. In addition, encapsulating TPFPP into a L7EB1-modified lactosome without short photoirradiation did not successfully deliver the siRNA into cytosols, indicating that the mechanism of PCI is vital in the induction of endosomal/lysosomal membrane breakdown by photoactivation of the TPFPP that localizes on the membranes of these organelles. This observation indicates that the synergistic mechanism of the L7EB1/TPFPP/siRNA-lactosome complex system as a whole requires the incorporation of L7EB1 for cellular uptake efficiency and the PCI[30] of TPFPP for the photo-induced endosomal release[31] of siRNA into the cytosol. In our case, it is obvious that the two therapies operate sequentially, rather than in parallel to activate the gene transfection process. Therefore, in this study, an efficient, size controllable

siRNA delivery system was developed using the biodegradable and bioreducible L7EB1/TPFPP/siRNA-lactosome conjugate with suitable PCI effects.

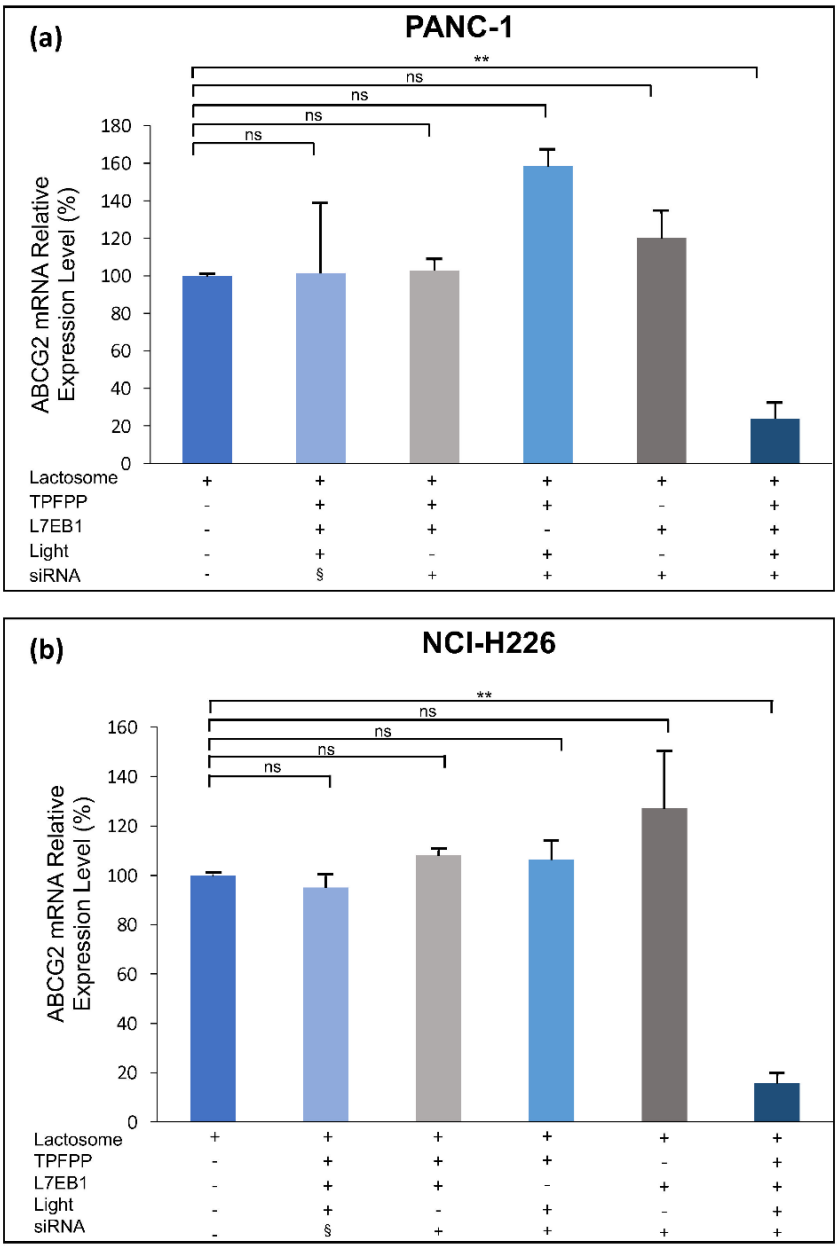

Fig. 4. *In vitro* ABCG2 knockdown analysis of various formulations of lactosome with siABCG2 incorporation on (a) PANC-1 and (b) NCI-H226 cell lines. § indicates scramble siRNA (siScr). The knockdown efficiency was measured after 48 h incubation. SPSS v.17 was used for statistical analysis. The *p* value: not significant (ns), $p<0.05$ (*) or $p<0.01$ (**). (n=3)

ALA mediated photo-induced cell death

One of the implications of PCI strategy is that the photosensitizers re-localize to other organelles, hence increasing phototoxicity[48] through the excitation of a membrane-bound photosensitizer to its singlet state. Therefore, the development of a potential siRNA carrier with negligible phototoxic and controllable properties for effective and efficient PCI-mediated gene delivery is warranted. MTT assays were performed on both PANC-1 and NCI-H226 cells to determine the toxicity effects of the L7EB1/TPFPP/siRNA-lactosome complex delivery systems on cell viability. Following light irradiation, the L7EB1/TPFPP/siScr-lactosome (with photoirradiation) and L7EB1/TPFPP/siABCG2-lactosome (with photoirradiation) treated PANC-1 cells displayed 93.0 ± 7.7% and 83.5 ± 10.5% cell viability, respectively, compared to the control-lactosome group (p=0.257 and p=0.113, respectively) as shown in Figure 5(a). While the L7EB1/TPFPP/siScr-lactosome (with photoirradiation) and L7EB1/TPFPP/siABCG2-lactosome (with photoirradiation) treated NCI-H226 cell line displayed 82.2 ± 8.9% and 80.7 ± 9.5% cell viability, respectively, compared to the control-lactosome group (p=0.074 and p=0.072, respectively), shown in Figure 5(b). These observations show that the photosensitizer L7EB1/TPFPP/siScr-lactosome and L7EB1/TPFPP/siABCG2-lactosome complexes did not exhibit any photo-induced cytotoxicity on their own, even after light irradiation using a continuous laser at 405 nm for 20 s. Moreover, L7EB1/TPFPP/siABCG2-lactosome (without photoirradiation) treated PANC-1 cells displayed 95.9 ± 2.1% cell viability compared to the control-lactosome group (p=0.078) while L7EB1/TPFPP/siABCG2-lactosome (without photoirradiation) treated NCI-H226 cells displayed 77.8 ± 15.0% cell viability compared to the control-lactosome group (p=0.125), indicating that the encapsulation of TPFPP without short photoirradiation does not induce dark phototoxicity in these cancer cell lines. L7EB1/siABCG2-lactosome (without photoirradiation) treated PANC-1 cells displayed 84.7 ± 7.1% cell viability compared to the control-lactosome group (p=0.066) while L7EB1/siABCG2-lactosome (without photoirradiation) treated NCI-H226 cells displayed 97.0 ± 7.3% cell viability compared to control-lactosome group (p=0.555), suggesting that the encapsulation of L7EB1 did not exhibit any toxic effect on its own. However, TPFPP/siABCG2-lactosome (with photoirradiation) treated PANC-1 cell line displayed 72.0 ± 8.0% cell viability, which was significantly lower compared to the control-lactosome group (p=0.026). One of the reasons for this may be due to the possibility that a fraction of the hydrophobic TPFPP, in the absence of L7EB1, may have an affinity towards the negatively charged plasma membrane instead. If so, the short photoirradiation induced the excited

TPFPP to generate ROS which possibly photodamaged the plasma membrane of the PANC-1 cells. On the contrary, this observation was not observed in the TPFPP/siABCG2-lactosome (with photoirradiation) treated NCI-H226 cell line which displayed a 92.0 ± 8.4% cell viability compared to the control-lactosome group (p=0.242) indicating that the observed TPFPP-cell membrane affinity may be cell specific.

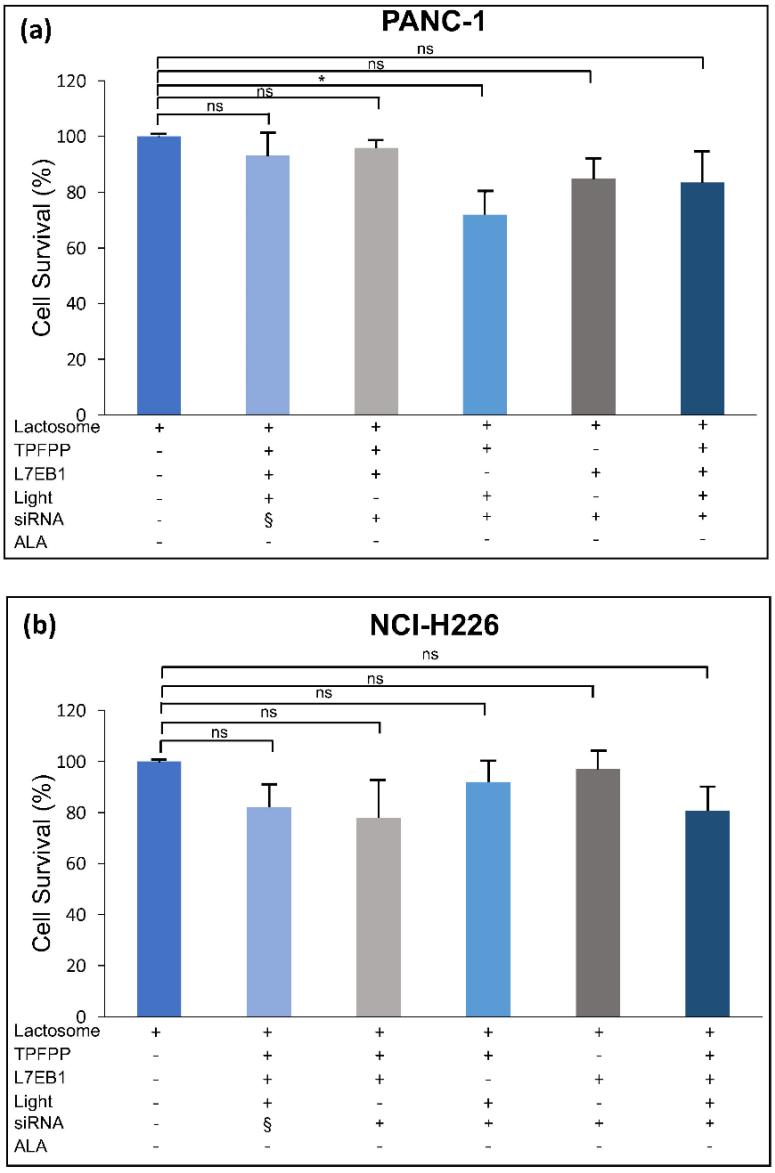

Fig. 5. The cytotoxic damage of various formulations of lactosome with siABCG2 incorporation on (a) PANC-1 and (b) NCI-H226 cell lines. § indicates scramble siRNA (siScr). SPSS v.17 was used for statistical analysis. The p value: not significant (ns), p<0.05 (*). (n=3)

A previous study, however, showed that photoinduced singlet oxygen generation from TPP photosensitizer-loaded lactosomes after irradiation at 405 nm for 50 s inducing significant cell death in cancer cells[15]. Another separate study reported a sharp increase of cytosolic fluorescence, indicating the release of the cargo from polyplexes after just 12.9 s of illumination with 405 nm light[31]. Therefore, by careful consideration of the photoirradiation exposure time, cytosolic release of siRNA is possible without significant cell damage induced by ROS generated lipid peroxidation. Therefore, with minimal toxicity light doses, we propose that the lactosome complex used in this experiment is a safe and efficient targeted delivery system for siRNA.

However, after 48 h of lactosome-complex transfection, when exogenous ALA was added to the treated cells coupled with PDT treatment, the L7EB1/TPFPP/siABCG2-lactosome treated PANC-1 cell line displayed 26.1 ± 14.4% cell viability compared to the control-lactosome group (p=0.012) as shown in Figure 6(a), while the L7EB1/TPFPP/siABCG2-lactosome treated NCI-H226 cell line displayed 61.1 ± 7.3% cell viability compared to the control-lactosome group (p=0.012), shown in Figure 6(b). The significant reduction of cell viability in both cell lines substantiates the negative correlation of protoporphyrin IX (PpIX) transporter ABCG2 expression level to ALA-mediated PpIX accumulation[27], and thereby facilitating the efficacy of PDT therapy[25] in cancer cells. Meanwhile, the L7EB1/siABCG2-lactosome (without photoirradiation) treated PANC-1 cells displayed 98.8 ± 1.6% cell viability compared to the control-lactosome group (p=0.326) while L7EB1/siABCG2-lactosome (without photoirradiation) treated NCI-H226 cells displayed 93.1 ± 20.4% cell viability compared to the control-lactosome group (p=0.616), which was consistent with the result that encapsulating L7EB1 alone was insufficient to deliver ABCG2 siRNA into the cytosol of both cancer cell lines for gene silencing, and hence unable to facilitate cell death via the ALA-mediated PpIX accumulated PDT effect. The L7EB1/TPFPP/siABCG2-lactosome (without photoirradiation) complex treated PANC-1 and NCI-H226 cells were 100.0 ± 3.1% and 98.6 ± 9.1% viable, respectively, compared to the control-lactosome complex treated cells (p=0.988 and p=0.820, respectively), indicating that without the PCI-induced ABCG2 gene silencing effect, the efficacy of the ALA-mediated PpIX accumulated PDT pathway was not promoted. However, L7EB1/TPFPP/siScr-lactosome (with photoirradiation) and TPFPP/siABCG2-lactosome (with photoirradiation) treated PANC-1 cells displayed 73.6 ± 9.7% and 86.3 ± 4.2% cell viability, respectively, both significantly lower compared to the control-lactosome group (p=0.043 and p=0.03, respectively). There were several factors substantiating this observation: (i) The effect of ALA-mediated PpIX

accumulated PDT via photo-induced cell death, in addition to the excited plasma membrane bound-TPFPP (in the absence of L7EB1) induced by short photoirradiation, generated ROS causing significant cell death in the PANC-1 cell line. (ii) The additive effect of PDT from ALA-mediated PpIX and PCI effect from TPFPP/lactosome complexes, both involving porphyrin derivatives, when excited, was capable of generating ROS which caused the cell membrane and endosomal membrane to rupture and induce cell death in the PANC-1 cell line. (iii) The observed photosensitive nature of the PANC-1 cell line towards PDT and PCI effects was not displayed by the NCI-H226 cell line. The L7EB1/TPFPP/siScr-lactosome (with photoirradiation) and TPFPP/siABCG2-lactosome (with photoirradiation) treated NCI-H226 cells displayed 82.2 ± 8.9% and 92.0 ± 8.4% cell viability, respectively, compared to the control-lactosome group (p=0.074 and p=0.242, respectively).

Overall, we claim that the major reduction of cell viability is via the PDT 10 min illumination with a 630 nm light and not via the PCI effect in this experiment. Moreover, previous studies have reported that photochemical treatment using photosensitizers such as ALA-mediated PpIX that does not localize in endocytic vesicles do not facilitate transfection, irrespective of DDS type. In contrast, only photosensitizers demonstrating endocytic vesicle affinity, such as the TPFPP used in our case, significantly increase transfection efficiency[49]. Therefore, in this study, the delivered siABCG2 not only exhibited a gene silencing effect in the cytosol but also provided a platform for ALA-mediated PpIX accumulated PDT via photo-induced cell death. For both PCI and PDT of cancer to be translated *in vivo*, the main drawback is the limited penetration of light to the tissue. However, with recent advancement in technologies, a combination of an ultraviolet-weighted spectrum of radioactive decay called Cherenkov luminescence (CL) and biomedical nanoparticles may improve future diagnosis and therapy, especially in the oncological field[50]. The biodegradable and size modifiable A_3B-type lactosome provides promising prospects for metal nuclide conjugation[51]. Therefore, future studies involving *in vivo* transfection and ALA-mediated PDT with light irradiation should be encouraged.

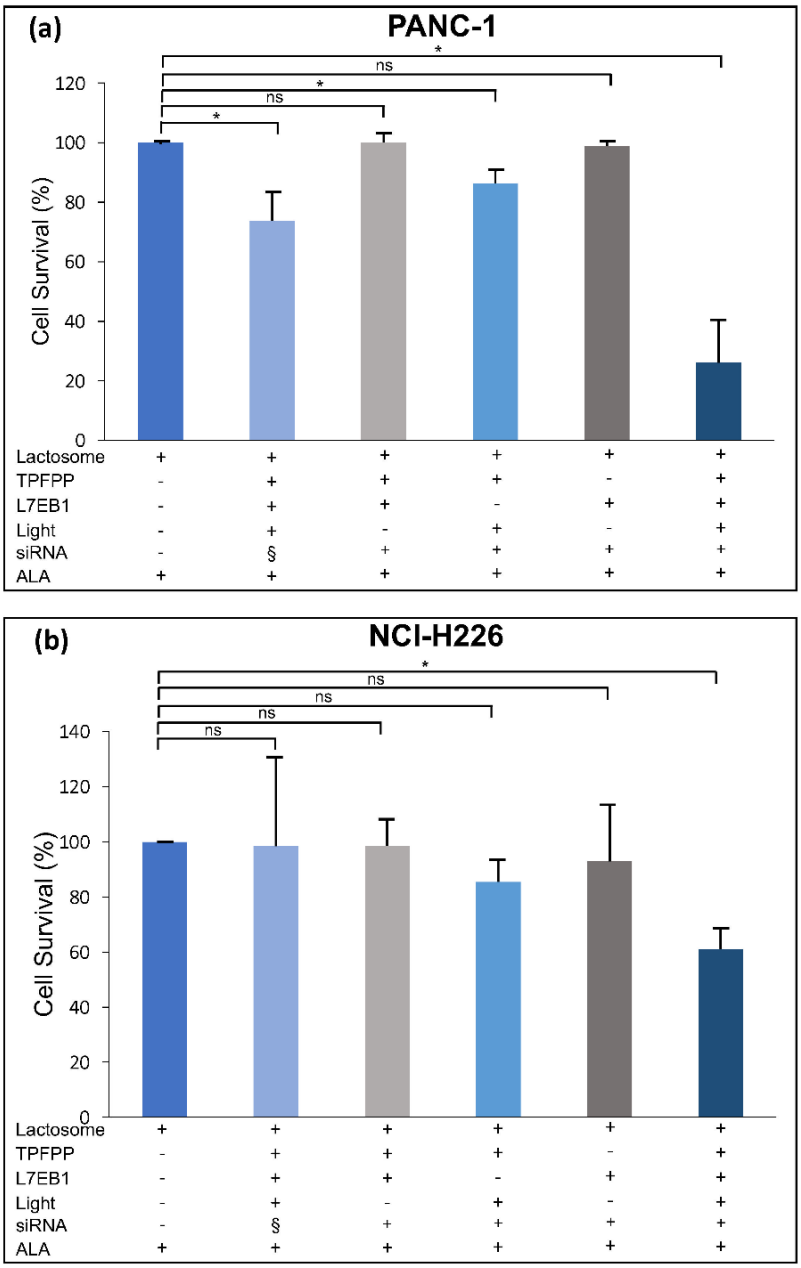

Fig. 6. The cytotoxic damage of various formulations of lactosome with siABCG2 treated with ALA-PDT on (a) PANC-1 and (b) NCI-H226 cell lines. Following 48 h incubation after lactosome-complex transfection, cells were exposed to light (40 mW/cm^2) for 10 minutes using a Na-Li lamp after 3 h incubation with 1 mM ALA. Twenty-four h after irradiation, the MTT assay was performed. § indicates scramble siRNA (siScr). SPSS v.17 was used for statistical analysis. The *p* value: not significant (ns), $p<0.05$ (*). (n=3).

Conclusion

The cell penetrating peptide-modified A_3B-type lactosome complex was conjugated with siRNA for cellular uptake and gene silencing effects. However, because the siRNAs are not readily dispersed into the perinuclear region or cytosol, photosensitizers were loaded into the lactosomes. Of the five types of photosensitizers tested (TPFPP, TPP, protoporphyrin IX, phloxine B and rhodamine 6G), TPFPP showed the highest degree of photoinduced cytosolic dispersion. The L7EB1/TPFPP/siRNA-lactosome complex efficiently knocked down the ABCG2 gene expression in PANC-1 and NCI-H226 cell lines via L7EB1 enhanced cellular uptake and TPFPP-guided photochemical-internalized cytosolic dispersion. Further gene silencing may be achieved through a modification of the TPFPP concentration and/or by changing the short photoirradiation exposure time.

Here, we have developed a safe and efficient siRNA delivery system via PCI-improved cytosolic release of siRNA with minimal cell toxicity shown in an MTT analysis. The bioreducible and size modifiable nature of the A_3B-type lactosome provides superiority over other micelleplexes in terms of safety and stability, which are imperative for therapeutic nanoparticles. Furthermore, a stable conjugated polyplex is highly favored compared to a supramolecular approach. Moreover, the L7EB1/TPFPP/siRNA-lactosome complex, while exhibiting an ABCG2 gene silencing effect in the cytosol, catalysed photo-induced cell death via ALA-mediated PpIX accumulated PDT. Overall, these proof-of-concept findings provide rudimentary value in spearheading a new approach in synergistic treatment for recalcitrant cancer cells through the integration of PDT and gene silencing.

Conflicts of interest

There are no conflicts to declare.

Acknowledgements

This study was supported by a grant from the Japan Agency for Medical Research and Development, Project for Cancer Research and Therapeutic Evolution (P-DIRECT and P-CREATE). We thank S. Inokawa and M. Ohshima (Okayama University) for their preliminary studies of the siRNA-loaded lactosome preparation.

References

1. Wang J, Lu Z, Wientjes MG, Au JL 2010. Delivery of siRNA therapeutics: barriers and carriers. AAPS J 12(4):492-503.
2. Qu MH, Zeng RF, Fang S, Dai QS, Li HP, Long JT 2014. Liposome-based co-delivery of siRNA and docetaxel for the synergistic treatment of lung cancer. Int J Pharm 474(1-2):112-122.
3. Zuckerman JE, Davis ME 2015. Clinical experiences with systemically administered siRNA-based therapeutics in cancer. Nat Rev Drug Discov 14(12):843-856.
4. Xu X, Wu J, Liu Y, Saw PE, Tao W, Yu M, Zope H, Si M, Victorious A, Rasmussen J, Ayyash D, Farokhzad OC, Shi J 2017. Multifunctional envelope-type siRNA delivery nanoparticle platform for prostate cancer therapy. ACS Nano 11(3):2618-2627.
5. Hussein WM, Cheong YS, Liu C, Liu G, Begum AA, Attallah MA, Moyle PM, Torchilin VP, Smith R, Toth I 2019. Peptide-based targeted polymeric nanoparticles for siRNA delivery. Nanotechnology 30(41):415604.
6. Whitehead KA, Langer R, Anderson DG 2009. Knocking down barriers: advances in siRNA delivery. Nat Rev Drug Discov 8(2):129-138.
7. Huang C, Li M, Chen C, Yao Q 2008. Small interfering RNA therapy in cancer: mechanism, potential targets, and clinical applications. Expert Opin Ther Targets 12(5):637-645.
8. Hong CA, Nam YS 2014. Functional nanostructures for effective delivery of small interfering RNA therapeutics. Theranostics 4(12):1211-1232.
9. Patel NR, Pattni BS, Abouzeid AH, Torchilin VP 2013. Nanopreparations to overcome multidrug resistance in cancer. Adv Drug Deliv Rev 65(13-14):1748-1762.
10. Shi J, Xiao Z, Votruba AR, Vilos C, Farokhzad OC 2011. Differentially charged hollow core/shell lipid-polymer-lipid hybrid nanoparticles for small interfering RNA delivery. Angew Chem Int Ed Engl 50(31):7027-7031.
11. Chen Y, Li J, Oupicky D 2018. Conjugate Polyplexes with anti-invasive properties and Improved siRNA Delivery In Vivo. Bioconjug Chem 29(2):296-305.
12. Wang Y, Wei G, Zhang X, Xu F, Xiong X, Zhou S 2017. A Step-by-step multiple stimuli-responsive nanoplatform for enhancing combined chemo-photodynamic therapy. Adv Mater 29(12):1605357.

13. Gao Y, Liu XL, Li XR 2011. Research progress on siRNA delivery with nonviral carriers. Int J Nanomedicine 6:1017-1025.

14. Makino A, Yamahara R, Ozeki E, Kimura S 2007. Preparation of novel polymer assemblies, "lactosome", composed of poly(L-lactic acid) and poly(sarcosine). Chemistry Letters 36(10):1220-1221.

15. Akahoshi A, Matsuura E, Ozeki E, Matsui H, Watanabe K, Ohtsuki T 2016. Enhanced cellular uptake of lactosomes using cell-penetrating peptides. Sci Technol Adv Mater 17(1):245-252.

16. Hara E, Makino A, Kurihara K, Yamamoto F, Ozeki E, Kimura S 2012. Pharmacokinetic change of nanoparticulate formulation "Lactosome" on multiple administrations. Int Immunopharmacol 14(3):261-266.

17. Hara E, Ueda M, Kim CJ, Makino A, Hara I, Ozeki E, Kimura S 2014. Suppressive immune response of poly-(sarcosine) chains in peptide-nanosheets in contrast to polymeric micelles. J Pept Sci 20(7):570-577.

18. Fang J, Nakamura H, Maeda H 2011. The EPR effect: Unique features of tumor blood vessels for drug delivery, factors involved, and limitations and augmentation of the effect. Adv Drug Deliv Rev 63(3):136-151.

19. Hara E, Ueda M, Makino A, Hara I, Ozeki E, Kimura S 2014. Factors influencing in vivo disposition of polymeric micelles on multiple administrations. ACS Med Chem Lett 5(8):873-877.

20. Makino A, Kizaka-Kondoh S, Yamahara R, Hara I, Kanzaki T, Ozeki E, Hiraoka M, Kimura S 2009. Near-infrared fluorescence tumor imaging using nanocarrier composed of poly(L-lactic acid)-block-poly(sarcosine) amphiphilic polydepsipeptide. Biomaterials 30(28):5156-5160.

21. Meyer M, Dohmen C, Philipp A, Kiener D, Maiwald G, Scheu C, Ogris M, Wagner E 2009. Synthesis and biological evaluation of a bioresponsive and endosomolytic siRNA-polymer conjugate. Mol Pharm 6(3):752-762.

22. Park K, Yang JA, Lee MY, Lee H, Hahn SK 2013. Reducible hyaluronic acid-siRNA conjugate for target specific gene silencing. Bioconjug Chem 24(7):1201-1209.

23. Mao Q, Unadkat JD 2015. Role of the breast cancer resistance protein (BCRP/ABCG2) in drug transport--an update. AAPS J 17(1):65-82.

24. Horsey AJ, Cox MH, Sarwat S, Kerr ID 2016. The multidrug transporter ABCG2: still more questions than answers. Biochem Soc Trans 44(3):824-830.

25. Susanto J, Lin YH, Chen YN, Shen CR, Yan YT, Tsai ST, Chen CH, Shen CN 2008. Porphyrin homeostasis maintained by ABCG2 regulates self-renewal of embryonic stem cells. PLoS One 3(12):e4023.

26. Jonker JW, Buitelaar M, Wagenaar E, Van Der Valk MA, Scheffer GL, Scheper RJ, Plosch T, Kuipers F, Elferink RP, Rosing H, Beijnen JH, Schinkel AH 2002. The breast cancer resistance protein protects against a major chlorophyll-derived dietary phototoxin and protoporphyria. Proc Natl Acad Sci U S A 99(24):15649-15654.

27. Kobuchi H, Moriya K, Ogino T, Fujita H, Inoue K, Shuin T, Yasuda T, Utsumi K, Utsumi T 2012. Mitochondrial localization of ABC transporter ABCG2 and its function in 5-aminolevulinic acid-mediated protoporphyrin IX accumulation. PLoS One 7(11):e50082.

28. Dougherty TJ, Gomer CJ, Henderson BW, Jori G, Kessel D, Korbelik M, Moan J, Peng Q 1998. Photodynamic therapy. J Natl Cancer Inst 90(12):889-905.

29. Selbo PK, Hogset A, Prasmickaite L, Berg K 2002. Photochemical internalisation: a novel drug delivery system. Tumour Biol 23(2):103-112.

30. Shieh MJ, Peng CL, Lou PJ, Chiu CH, Tsai TY, Hsu CY, Yeh CY, Lai PS 2008. Non-toxic phototriggered gene transfection by PAMAM-porphyrin conjugates. J Control Release 129(3):200-206.

31. de Bruin KG, Fella C, Ogris M, Wagner E, Ruthardt N, Brauchle C 2008. Dynamics of photoinduced endosomal release of polyplexes. J Control Release 130(2):175-182.

32. Berg K, Dietze A, Kaalhus O, Hogset A 2005. Site-specific drug delivery by photochemical internalization enhances the antitumor effect of bleomycin. Clin Cancer Res 11(23):8476-8485.

33. Prasmickaite L, Cekaite L, Hellum M, Hovig E, Hogset A, Berg K 2006. Transcriptome changes in a colon adenocarcinoma cell line in response to photochemical treatment as used in photochemical internalisation (PCI). FEBS Lett 580(24):5739-5746.

34. Weyergang A, Selbo PK, Berg K 2006. Photochemically stimulated drug delivery increases the cytotoxicity and specificity of EGF-saporin. J Control Release 111(1-2):165-173.

35. Prasmickaite L, Hogset A, Selbo PK, Engesaeter BO, Hellum M, Berg K 2002. Photochemical disruption of endocytic vesicles before delivery of drugs: a new strategy for cancer therapy. Br J Cancer 86(4):652-657.

36. Folini M, Berg K, Millo E, Villa R, Prasmickaite L, Daidone MG, Benatti U, Zaffaroni N 2003. Photochemical internalization of a peptide nucleic acid targeting the catalytic subunit of human telomerase. Cancer Res 63(13):3490-3494.

37. Lai PS, Lou PJ, Peng CL, Pai CL, Yen WN, Huang MY, Young TH, Shieh MJ 2007. Doxorubicin delivery by polyamidoamine dendrimer conjugation and photochemical internalization for cancer therapy. J Control Release 122(1):39-46.

38. Shimizu Y, Temma T, Hara I, Makino A, Yamahara R, Ozeki E, Ono M, Saji H 2014. Micelle-based activatable probe for in vivo near-infrared optical imaging of cancer biomolecules. Nanomedicine 10(1):187-195.

39. Amo T, Kawanishi N, Uchida M, Fujita H, Oyanagi E, Utsumi T, Ogino T, Inoue K, Shuin T, Utsumi K, Sasaki J 2009. Mechanism of cell death by 5-aminolevulinic acid-based photodynamic action and its enhancement by ferrochelatase inhibitors in human histiocytic lymphoma cell line U937. Cell Biochem Funct 27(8):503-515.

40. Lee SH, Kang YY, Jang HE, Mok H 2016. Current preclinical small interfering RNA (siRNA)-based conjugate systems for RNA therapeutics. Adv Drug Deliv Rev 104:78-92.

41. An X, Zhu A, Luo H, Ke H, Chen H, Zhao Y 2016. Rational design of multi-stimuli-responsive nanoparticles for precise cancer therapy. ACS Nano 10(6):5947-5958.

42. Such GK, Yan Y, Johnston AP, Gunawan ST, Caruso F 2015. Interfacing materials science and biology for drug carrier design. Adv Mater 27(14):2278-2297.

43. Zhang P, An K, Duan X, Xu H, Li F, Xu F 2018. Recent advances in siRNA delivery for cancer therapy using smart nanocarriers. Drug Discov Today 23(4):900-911.

44. Benmerah A, Lamaze C 2007. Clathrin-coated pits: vive la difference? Traffic 8(8):970-982.

45. Wang J, Byrne JD, Napier ME, DeSimone JM 2011. More effective nanomedicines through particle design. Small 7(14):1919-1931.

46. Berg K, Selbo PK, Prasmickaite L, Tjelle TE, Sandvig K, Moan J, Gaudernack G, Fodstad O, Kjolsrud S, Anholt H, Rodal GH, Rodal SK, Hogset A 1999. Photochemical internalization: a novel technology for delivery of macromolecules into cytosol. Cancer Res 59(6):1180-1183.

47. Laroui N, Coste M, Lichon L, Bessin Y, Gary-Bobo M, Pratviel G, Bonduelle C, Bettache N, Ulrich S 2019. Combination of photodynamic therapy and gene silencing achieved through the hierarchical self-assembly of porphyrin-siRNA complexes. International Journal of Pharmaceutics 569:118585.

48. Nishiyama N, Iriyama A, Jang WD, Miyata K, Itaka K, Inoue Y, Takahashi H, Yanagi Y, Tamaki Y, Koyama H, Kataoka K 2005. Light-induced gene transfer from packaged DNA enveloped in a dendrimeric photosensitizer. Nat Mater 4(12):934-941.

49. Prasmickaite L, Hogset A, Berg K 2001. Evaluation of different photosensitizers for use in photochemical gene transfection. Photochem Photobiol 73(4):388-395.

50. Shaffer TM, Pratt EC, Grimm J 2017. Utilizing the power of cerenkov light with nanotechnology. Nat Nanotechnol 12(2):106-117.

51. Kurihara K, Ueda M, Hara I, Ozeki E, Togashi K, Kimura S 2018. Polymeric micelle of A_3B-Type lactosome as a vehicle for targeting meningeal dissemination. Nanomaterials (Basel) 8(2): 79.

Supplementary Information for

Lactosome-conjugated siRNA nanoparticles for photo-enhanced gene silencing in cancer cells

Melissa Siaw Han Lim[a], Yuki Nishiyama[b], Takashi Ohtsuki[b]*, Kazunori Watanabe[b], Hirotsugu Kobuchi[a], Kazuko Kobayashi[a] and Eiji Matsuura[a,c,d]

[a]Department of Cell Chemistry, Graduate School of Medicine, Dentistry, and Pharmaceutical Sciences, Okayama University, 2-5-1 Shikata-cho, Kita-ku, Okayama 700-8558, Japan

[b]Department of Interdisciplinary Science and Engineering in Health Systems, Okayama University, 3-1-1 Tsushima-naka, Okayama 700-8530, Japan

[c]Neutron Therapy Research Centre, Okayama University, 2-5-1 Shikata-cho, Kita-ku, Okayama 700-8558, Japan

[d]Collaborative Research Centre for OMIC, Graduate School of Medicine, Dentistry, and Pharmaceutical Sciences, Okayama University, 2-5-1 Shikata-cho, Kita-ku, Okayama 700-8558, Japan

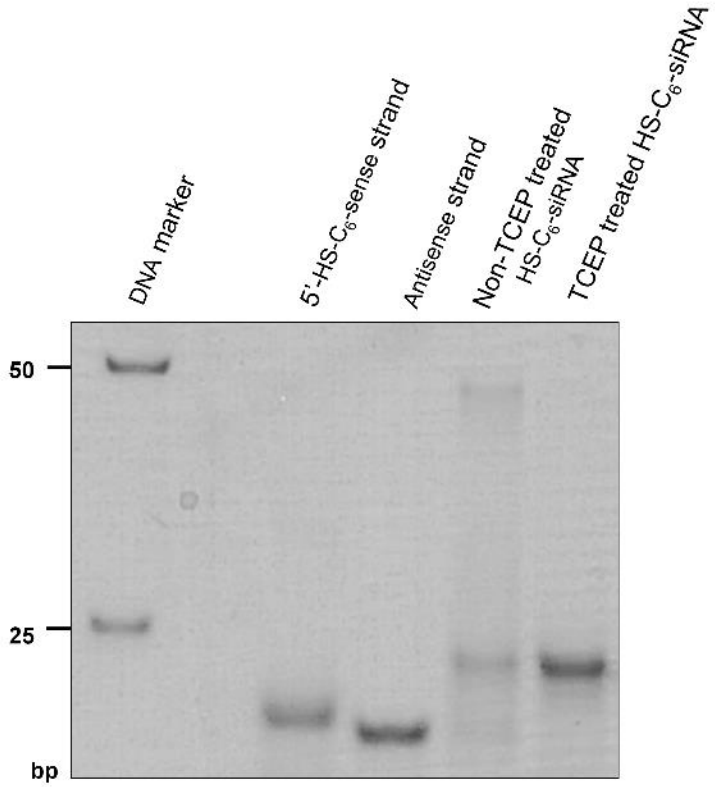

Figure S1. Native 10% PAGE analysis of TCEP treated HS-C_6-siRNA stained with 0.025% toluidine blue.

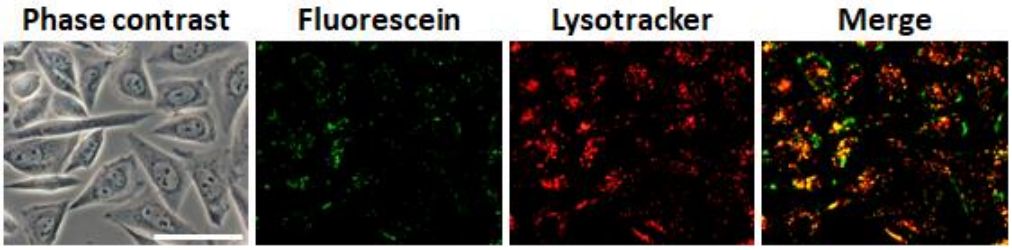

Figure S2. Endosomal entrapment of L7EB1/TPFPP-lactosome including PLLA-fluorescein (0.5 mol% of the lactosome polymer). CHO cells were treated with the lactosome as described in the Materials and Methods. The cells were stained with 50 nM Lysotracker Red (Thermo Fisher Scientific) at 37˚C for 30 min. Scale bar, 50 μm.